J. Fluid Mech. (1991), *vol.* 228, *pp.* 549–560
Printed in Great Britain

Wind-augmented transport and dilution in shallow-water flows

By RONALD SMITH

Department of Mathematical Sciences, University of Technology, Loughborough, LE11 3TU, UK

(Received 2 July 1990)

Wind blowing across shallow water contributes to secondary flow across a vertical section. For particles which are not neutrally buoyant the vertical sampling of the secondary flow is non-uniform: buoyant material drifts with the wind and slightly dense material is carried against the wind. This paper focuses attention on the joint dependence of the horizontal dilution rates upon the strength of the wind-augmented current and upon the vertical rise (or sinking) velocity of the particles. In strong wind the greatly enhanced mixing counterbalances the onshore drift and explains why shoreline pollution is not significantly correlated to the onshore wind.

1. Introduction

When wind blows across a river or estuary, flotsam tends to drift with the wind, while mobile sediment tends to be carried in the opposite direction. This difference in behaviour is attributable to the secondary flow driven by the wind: the surface water is dragged along in the direction of the wind stress and there is a compensating counterflow near the bed (see figure 1). If a mixture of materials with different rise (or sinking) velocities is released into the flow there will be a tendency for the species to separate out. The efficiency of this fractionation can be severely reduced by the horizontal diffusion of the individual constituents.

Longitudinal fractionation is the basis of several chemical analysis techniques and chemical manufacturing processes. For over 20 years theoretical chemists have known how to calculate the longitudinal dilution rate as a function of the transverse rise (or sinking) velocity (Giddings 1968). Transverse dispersion associated with secondary flows has nearly as long a pedigree. For a neutrally buoyant tracer Fischer (1969) demonstrated experimentally and calculated theoretically how the transverse mixing rate in a curved channel could be up to 10 times what one would expect in a straight channel. Here we combine the mathematical ingredients of these two classical papers and we show how to calculate the longitudinal, transverse and mixed shear dispersion coefficients as functions of both the rise (or sinking) velocity and the strength of the wind-augmented current. The key assumption underlying such analyses is that the horizontal dispersion takes place on a timescale which is long compared with the equilibrium time for vertical rise and diffusion.

In the final section of this paper a solution of the horizontal advection–diffusion equation is used to calculate the dependence of the shoreline pollution on the onshore wind drift. For light winds (weak onshore drift) buoyant material is carried towards the shore giving slightly increased pollution. However, for strong winds (strong onshore drift) the greatly enhanced transverse shear dispersion brings the shoreline pollution level back down again. This non-monotonic dependence upon wind

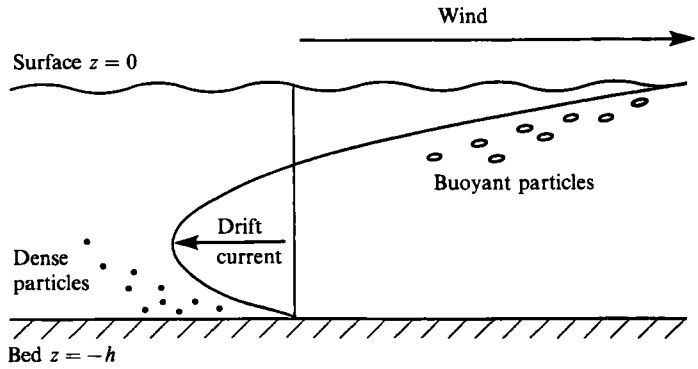

FIGURE 1. Sketch of the wind-driven velocity profile and the separation of buoyant and sinking particles.

strength is compatible with field observations that shoreline pollution is not significantly correlated with the onshore wind (Gameson, Bufton & Gould 1967).

2. Reaction–diffusion in shallow water

For simplicity we shall investigate the local shear dispersion process as if the flow properties (depth, velocities, diffusivities) were independent of the horizontal coordinates x, y. We regard the flow as being principally in the x-direction, with a wind-driven transverse flow. The particle concentration $c(x, y, z, t)$ is assumed to satisfy the reaction–diffusion equation

$$\partial_t c + u\,\partial_x c + v\,\partial_y c + \partial_z(wc) + \lambda c = \kappa_1 \partial_x^2 c + \kappa_2 \partial_y^2 c + \partial_z(\kappa_3 \partial_z c), \tag{2.1a}$$

with

$$wc - \kappa_3 \partial_z c = 0 \quad \text{on} \quad z = -h, 0. \tag{2.1b, c}$$

Here $u(z), v(z)$ are the horizontal particle velocities, $w(z)$ is the rise velocity, $\lambda(z)$ is the decay rate, and $\kappa_1(z), \kappa_2(z), \kappa_3(z)$ are the eddy diffusivities (in principal axes). The boundary conditions (2.1*b*, *c*) express the zero flux of tracer into the bed $z = -h$ and out of the free surface $z = 0$. The magnitude of the rise velocity w depends upon the size and density of the particles. The fluid velocities used to determine u, v are Reynolds-averaged velocities. For bacteria a non-uniform decay rate can arise from the penetration of sunlight into the water column. For reactive chemicals, uniform decay can result from oxygenation or other chemical reactions.

To make substantive use of the shallowness, we introduce a small parameter δ that characterizes the aspect ratio (depth to horizontal scale). Also, we use a frame of reference moving with horizontal velocity components U, V and we use a slow timescale T:

$$X = \delta(x - Ut), \quad Y = \delta(y - Vt), \quad T = \delta^2 t, \quad \Lambda = \lambda/\delta^2. \tag{2.2}$$

The appropriate values of U and V are calculated in the next section. With these changes the advection–diffusion equation takes the rescaled form

$$\delta^2 \partial_T c + \delta(u - U)\,\partial_X c + \delta(v - V)\,\partial_Y c + \partial_z(wc) + \delta^2 \Lambda c = \delta^2 \kappa_1 \partial_X^2 c + \delta^2 \kappa_2 \partial_Y^2 c + \partial_z(\kappa_3 \partial_z c). \tag{2.3}$$

In the limit as the aspect ratio δ tends to zero, the vertical concentration profile has the equilibrium shape

$$\gamma(z) = \exp\left(\int_{z_0}^{z} \frac{w}{\kappa_3} \mathrm{d}z' \right). \tag{2.4a}$$

A convenient choice for the reference level z_0 is to ensure that

$$\|\gamma\| = 1, \tag{2.4b}$$

where the vertical lines $\|\ldots\|$ denote a vertical average value. Thus, z_0 is merely the level at which γ equals its average value. If κ_3 tends to zero at the bed, then γ has a power-law singularity (Smith 1986).

Following Giddings (1968) we make direct allowance for the non-uniform sapling of the flow by representing the concentration

$$c = \gamma b. \tag{2.5}$$

The advection–diffusion equation for $b(X, Y, z, T)$ is

$$\delta^2\gamma\,\partial_T b + \delta\gamma(u-U)\,\partial_X b + \delta\gamma(v-V)\,\partial_Y b + \delta^2\Lambda\gamma b = \delta^2\gamma\kappa_1\,\partial_X^2 b + \delta^2\kappa_2\,\partial_Y^2 b + \partial_z(\gamma\kappa_3\,\partial_z c), \tag{2.6a}$$

with

$$\gamma\kappa_3\,\partial_z b = 0 \quad \text{on} \quad z = -h, 0. \tag{2.6b, c}$$

What has been achieved by the change of variables (2.5) is the elimination of vertical drift w, at the price of γ-weight factors associated with all the velocity and diffusivity terms.

3. Formal series expansion

The presence of the aspect-ratio parameter δ allows us to formalize the heuristic calculations first given by G. I. Taylor (1953) and later modified by Giddings (1968) and by Fischer (1969). For small δ we pose the regular power series expansion

$$b(X, Y, z, T) = \|b\| + \delta b^{(1)} + \delta^2 b^{(2)} + \ldots. \tag{3.1}$$

The leading term $\|b\|$ is vertically uniform (i.e. the non-uniform vertical structure is already accommodated via the equilibrium concentration profile γ).

The terms of order δ in (2.6*a*, *b*, *c*) yield equations satisfied by $b^{(1)}$:

$$\partial_z(\gamma\kappa_3\,\partial_z b^{(1)}) = \gamma(u-U)\,\partial_X\|b\| + \gamma(v-V)\,\partial_Y\|b\|, \tag{3.2a}$$

with

$$\gamma\kappa_3\,\partial_z b^{(1)} = 0 \quad \text{on} \quad z = -h, 0. \tag{3.2b, c}$$

By virtue of the boundary conditions (3.2*b*, *c*) the left-hand side of (3.2*a*) has zero vertical integral. For consistency the right-hand side terms must have the same property. This forces us to specify the velocity components U, V of the moving frame of reference

$$U = \|\gamma u\|, \quad V = \|\gamma v\|. \tag{3.3a, b}$$

In any other frame of reference there is not the hypothesized slow time evolution.

With these values for U, V a first integral for $b^{(1)}$ is

$$\partial_z b^{(1)} = \frac{1}{\gamma\kappa_3}\int_{-h}^{z}\gamma(u-U)\,\mathrm{d}z'\,\partial_X\|b\| + \frac{1}{\gamma\kappa_3}\int_{-h}^{z}\gamma(v-V)\,\mathrm{d}z'\,\partial_Y\|b\|. \tag{3.4a, b}$$

For later use we note the identifies (corresponding to integration by parts)

$$\|\gamma(u-U)\,b^{(1)}\| = -\|\partial_z b^{(1)}\int_{-h}^{z}\gamma(u-U)\,\mathrm{d}z'\|, \tag{3.5a}$$

$$\|\gamma(v-V)\,b^{(1)}\| = -\|\partial_z b^{(1)}\int_{-h}^{z}\gamma(v-V)\,\mathrm{d}z'\|. \tag{3.5b}$$

Our objective is to determine the slow horizontal evolution of $\|b\|$. If we take the terms of order-δ^2 in (2.6a, b, c) and average over the depth, then we obtain the horizontal evolution equation

$$\partial_T\|b\| + \|\gamma(u-U)\,\partial_X b^{(1)}\| + \|\gamma(v-V)\,\partial_Y b^{(1)}\| + \|\gamma\Lambda\|\,\|b\| = \|\gamma\kappa_1\|\partial_X^2\|b\| + \|\gamma\kappa_2\|\partial_Y^2\|b\|. \tag{3.6}$$

Equations (3.4), (3.5) enable us to replace the $b^{(1)}$ terms by $\partial_X\|b\|$, $\partial_Y\|b\|$ terms. The resulting horizontal evolution equation can be written

$$\partial_T\|b\| + \|\gamma\Lambda\|\,\|b\| = \{D_{11} + \|\gamma\kappa_1\|\}\,\partial_X^2\|b\| + \{D_{22} + \|\gamma\kappa_2\|\}\,\partial_Y^2\|b\| + 2D_{12}\,\partial_X\,\partial_Y\|b\|. \tag{3.7}$$

The components D_{ij} of the shear dispersion tensor have the integral representations

$$D_{11} = \left\| \frac{1}{\gamma\kappa_3}\left[\int_{-h}^{z}\gamma(u-U)\,\mathrm{d}z'\right]^2 \right\|, \tag{3.8a}$$

$$D_{22} = \left\| \frac{1}{\gamma\kappa_3}\left[\int_{-h}^{z}\gamma(v-V)\,\mathrm{d}z'\right]^2 \right\|, \tag{3.8b}$$

$$D_{12} = D_{21} = \left\| \frac{1}{\gamma\kappa_3}\left[\int_{-h}^{z}\gamma(u-U)\,\mathrm{d}z'\right]\left[\int_{-h}^{z}\gamma(v-V)\,\mathrm{d}z'\right] \right\|. \tag{3.8c}$$

In the appropriate one-dimensional or neutrally buoyant limiting cases these formulae (3.8a, b, c) are equivalent to the results derived by Giddings (1968, equation 19) and Fischer (1969, equation 6). If κ_3 tends to zero at the bed there are integrable singularities (Elder 1959; Smith 1986).

4. Shear dispersion equation

If we revert to the original coordinates x, y, t, then the vertically averaged concentration $\|c\|$ satisfies the two-dimensional shear dispersion equation

$$\partial_t\|c\| + \|\gamma u\|\partial_x\|c\| + \|\gamma v\|\partial_y\|c\| + \|\gamma\lambda\|\,\|c\|$$

$$= \{D_{11} + \|\gamma\kappa_1\|\}\,\partial_x^2\|c\| + \{D_{22} + \|\gamma\kappa_2\|\}\,\partial_y^2\|c\| + 2D_{12}\,\partial_x\,\partial_y\|c\|. \tag{4.1}$$

The presence of the equilibrium vertical concentration profile $\gamma(z)$ reveals how constituents with different rise (or sinking) velocities are moved at different horizontal velocities. Also, via γ in the formula (3.8a, b, c) for the shear dispersion components, we see that the different constituents experience different rates of dilution.

As was emphasized by Taylor (1953), the shear dispersion coefficients D_{ij} depend inversely upon the vertical rate of mixing κ_3. So, if the diffusivities κ_i are small then it requires very little velocity shear for the shear dispersion to dominate. For turbulent flows κ_i scale as hu_*, where u_* is the friction or shear velocity. Elder (1959) showed that in the longitudinal direction shear dispersion dominates turbulence by a factor of 40. So from the quadratic dependence of D_{22} upon the transverse velocities, we can infer that in the transverse direction it only needs a drift current of about $40^{-\frac{1}{2}}$ of the friction velocity for transverse shear dispersion to match the transverse turbulence.

In practice the flow properties (depth, velocities, diffusivities and the equilibrium vertical concentration profile γ) are functions of horizontal position x, y. So, the

construction of the moving coordinate system X, Y would require a more complicated Lagrangian type of definition (Smith 1983). The appropriate generalization of the constant coefficient equation (4.1) is

$$\begin{aligned}\partial_t(h\|c\|)+\partial_x(h\|\gamma u\|\,\|c\|)+\partial_y(h\|\gamma v\|\,\|c\|)+h\|\gamma\lambda\|\,\|c\| \\ = \partial_x(h[D_{11}+\|\gamma\kappa_1\|]\partial_x\|c\|)+\partial_y(h[D_{22}+\|\gamma\kappa_2\|]\partial_y\|c\|) \\ +\partial_x(hD_{12}\partial_y\|c\|)+\partial_y(hD_{21}\partial_x\|c\|).\end{aligned} \tag{4.2}$$

When the decay rate λ is zero, this equation is in conservation form. So, quite properly, there is then no loss of tracer.

5. Constant-viscosity model

For realistic flows the integral formulae (3.8*a*, *b*, *c*) for the shear dispersion coefficients would need to be evaluated numerically (Fischer 1969; Smith 1986). Moreover, the coefficients D_{ij} depend nonlinearly upon the velocity components. So, there is not simple linear superposition of the effects of wind and the tidal current. Nevertheless, there is didactic advantage in considering an exactly solvable idealization. The chosen example is the effect of surface stresses on a constant-viscosity and constant-diffusivity flow. This conforms closely to the numerical investigation by Munro & Mollowney (1974).

For a shallow flow the dominant terms in the horizontal momentum equations are

$$\mu\,\partial_z^2 u = \partial_x\|p\|, \tag{5.1a}$$

$$\mu\,\partial_z^2 v = \partial_y\|p\|, \tag{5.1b}$$

with
$$u = v = 0 \quad \text{at} \quad z = -h, \tag{5.1c}$$

and
$$\mu\,\partial_z u = \tau_1, \quad \mu\,\partial_z v = \tau_2 \quad \text{at} \quad z = 0. \tag{5.1d, e}$$

Here μ is the constant viscosity, $\|p\|$ is the vertically averaged dynamic pressure, and τ_1, τ_2 are the components of wind stress acting at the upper surface (within about one water depth of a boundary, horizontal velocity gradients $\partial_x^2 u, \partial_y^2 u$ would need to be included).

It is convenient to decompose the velocity field into contributions associated with the bulk flow $\|u\|, \|v\|$ and with the surface stresses. The solutions of (5.1*a*–*e*) can be written

$$u = \|u\|3\xi(1-\tfrac{1}{2}\xi)+\hat{u}(3\xi^2-2\xi), \tag{5.2a}$$

$$v = \|v\|3\xi(1-\tfrac{1}{2}\xi)+\hat{v}(3\xi^2-2\xi), \tag{5.2b}$$

with
$$\xi = 1+\frac{z}{h}, \quad \hat{u} = \frac{\tau_1 h}{4\mu}, \quad \hat{v} = \frac{\tau_2 h}{4\mu}. \tag{5.2c, d, e}$$

Hence, we characterize the wind stresses τ_1, τ_2 in terms of the surface drift velocities $\hat{u}, \hat{v}$. Figure 2 shows the relative shapes of the velocity profiles for the bulk flow and surface drift contributions to the flow.

For the purposes of the present paper we shall regard the quantities $\|u\|$, $\|v\|$, $\hat{u}$, $\hat{v}$ as being given. For completeness, we record that for the velocity components (5.2*a*, *b*) to satisfy the momentum equations (5.1 *a*, *b*) the pressure gradient must be related to the wind stresses and bulk flow:

$$\tfrac{2}{3}\partial_x\|p\| = \frac{\tau_1}{h}-\mu\frac{\|u\|}{h^2}, \tag{5.3a}$$

$$\tfrac{2}{3}\partial_y\|p\| = \frac{\tau_2}{h}-\mu\frac{\|v\|}{h^2}. \tag{5.3b}$$

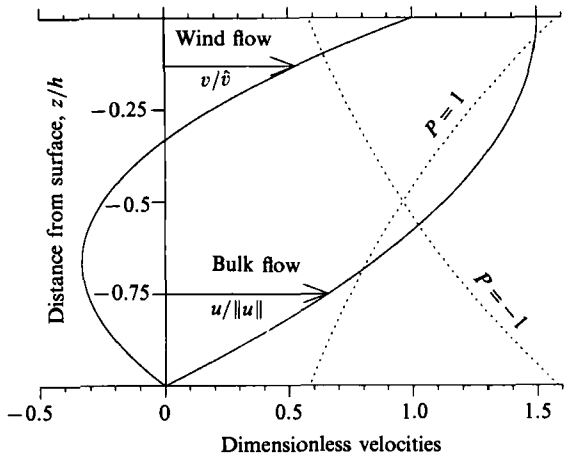

FIGURE 2. Velocity profiles of the bulk flow and wind-driven flow. The dotted curves show the equilibrium concentration profiles for buoyant ($P = 1$) and for sinking ($P = -1$) particles.

These equations are valid on horizontal lengthscales greater than the water depth. As with Euler's equation there can be no normal flow across a boundary, but slip is permitted.

6. Effective horizontal velocities U, V

For particles with constant rise velocity w and constant vertical diffusivity κ_3 the equilibrium concentration profile γ is given by

$$\gamma = \frac{P\exp(P\xi)}{\exp(P)-1}, \tag{6.1a}$$

with

$$P = \frac{wh}{\kappa_3}, \quad \xi = 1+\frac{z}{h}. \tag{6.1b, c}$$

The vertical Péclet number P is positive for a rising substance and negative for a sinking substance. Figure 2 includes the equilibrium concentration profiles of γ for $P = -1, 1$.

We are now in a position to quantify the different effective horizontal velocities (3.3a, b) experienced by rising and sinking substances:

$$U = \frac{3\|u\|}{2(\exp(P)-1)}\left\{\exp(P)\left[1-\frac{2}{P^2}\right]+\frac{2}{P}+\frac{2}{P^2}\right\} + \frac{\hat{u}}{\exp(P)-1}\left\{\exp(P)\left[1-\frac{4}{P}+\frac{6}{P^2}\right]-\frac{2}{P}-\frac{6}{P^2}\right\}, \tag{6.2a}$$

$$V = \frac{3\|v\|}{2(\exp(P)-1)}\left\{\exp(P)\left[1-\frac{2}{P^2}\right]+\frac{2}{P}+\frac{2}{P^2}\right\} + \frac{\hat{v}}{\exp(P)-1}\left\{\exp(P)\left[1-\frac{4}{P}+\frac{6}{P^2}\right]-\frac{2}{P}-\frac{6}{P^2}\right\}. \tag{6.2b}$$

Despite appearances, there are no singularities at $P = 0$.

Figure 3 shows the P-dependence of the bulk flow and surface drift contributions to the effective horizontal velocity. The curves have been plotted in a way which gives emphasis to the quantitative similarity with the velocity profiles shown in

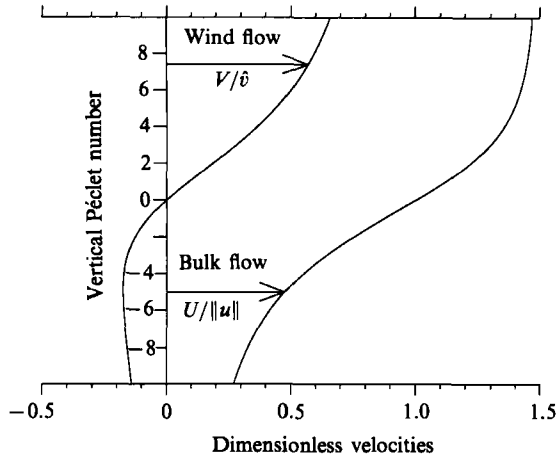

FIGURE 3. The scale-up factors for the contributions of the bulk flow and of the wind-driven current evaluated at the free surface towards the total effective horizontal velocity of rising or sinking particles.

figure 2 (i.e. buoyant particles tend to move with the surface water and dense particles tend to move with the bottom water).

7. Evaluating the shear dispersion tensor

The decomposition (5.2*a*, *b*) of the velocity into bulk-flow and wind-drift contributions encourages us to write

$$\int_{-h}^{z} \gamma(u-U)\,\mathrm{d}z' = h\|u\|\,I(\xi)+h\hat{u}\hat{I}(\xi), \tag{7.1a}$$

$$\int_{-h}^{z} \gamma(v-V)\,\mathrm{d}z' = h\|v\|\,I(\xi)+h\hat{v}\hat{I}(\xi), \tag{7.1b}$$

where

$$I(\xi) = \frac{3}{2(\exp(P)-1)}\left\{\exp(P\xi)\left[2\xi-\xi^2+\frac{2\xi-2}{P}-\frac{2}{P^2}\right]+\frac{2}{P}+\frac{2}{P^2}\right\}$$
$$-\frac{3(\exp(P\xi)-1)}{2(\exp(P)-1)^2}\left\{\exp(P)\left[1-\frac{2}{P^2}\right]+\frac{2}{P^2}+\frac{2}{P}+\frac{2}{P^2}\right\}, \tag{7.2a}$$

$$\hat{I}(\xi) = \frac{1}{(\exp(P)-1)}\left\{\exp(P\xi)\left[3\xi^2-2\xi+\frac{2-6\xi}{P}+\frac{6}{P^2}\right]-\frac{2}{P}-\frac{6}{P^2}\right\}$$
$$-\frac{(\exp(P\xi)-1)}{(\exp(P)-1)^2}\left\{\exp(P)\left[1-\frac{4}{P}+\frac{6}{P^2}\right]-\frac{2}{P}-\frac{2}{P^2}\right\}. \tag{7.2b}$$

In terms of the two functions $I, \hat{I}$ we define the bulk flow, wind drift, and mixed coefficients:

$$a_{\mathrm{B}}(P) = \frac{\exp(P)-1}{P}\int_0^1 \exp(-P\xi)\,I^2\,\mathrm{d}\xi, \tag{7.3a}$$

$$a_{\mathrm{W}}(P) = \frac{\exp(P)-1}{P}\int_0^1 \exp(-P\xi)\,\hat{I}^2\,\mathrm{d}\xi, \tag{7.3b}$$

$$a_{\mathrm{M}}(P) = \frac{\exp(P)-1}{P}\int_0^1 \exp(-P\xi)\,I\hat{I}\,\mathrm{d}\xi. \tag{7.3c}$$

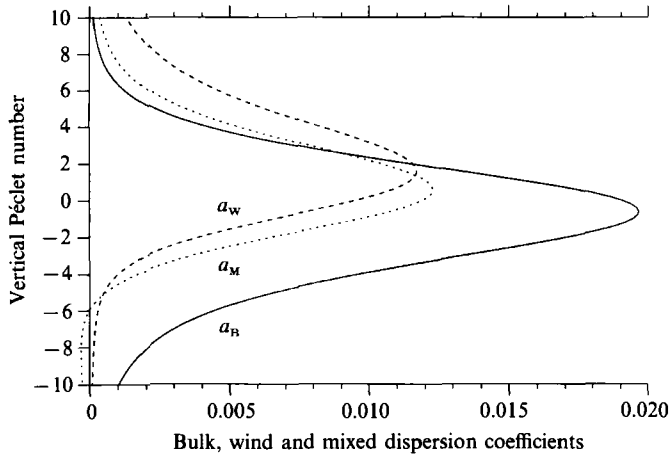

FIGURE 4. Weight factors a_B, a_W, a_M relating the magnitude of the horizontal shear dispersion to the bulk flow, wind-driven flow, and mixed terms.

The explicit formulae for the P-dependence of a_B, a_W and a_M are excessively lengthy. Instead, figure 4 plots the numerical values. The importance of these coefficients lies in the formulae for the shear dispersion tensor:

$$D_{11} = \frac{h^2}{\kappa_3}\{a_B\|u\|^2 + a_W\hat{u}^2 + 2a_M\|u\|\hat{u}\}, \tag{7.4a}$$

$$D_{22} = \frac{h^2}{\kappa_3}\{a_B\|v\|^2 + a_W\hat{v}^2 + 2a_M\|v\|\hat{v}\}, \tag{7.4b}$$

$$D_{12} = D_{21} = \frac{h^2}{\kappa_3}\{a_B\|u\|\,\|v\| + a_W\hat{u}\hat{v} + a_M(\|u\|\hat{v} + \|v\|\hat{u})\}. \tag{7.4c}$$

For the velocity profile associated with the bulk flow, the shear is largest near the bed. Accordingly, the bulk-flow coefficient a_B attains its maximum for a sinking tracer (with a negative value of P). Conversely, the velocity profile associated with the wind drift has strong shear at the surface, and the wind-drift coefficient a_W attains its maximum for a rising tracer.

In the neutrally buoyant case ($P = 0$) it is an elementary task to evaluate the integrals (7.1), (7.3) and to obtain the coefficients

$$a_B = \tfrac{2}{105}, \quad a_W = \tfrac{1}{105}, \quad a_M = \tfrac{1}{84} \quad \text{for} \quad P = 0. \tag{7.5a, b, c}$$

8. Insensitivity of shoreline pollution to wind strength

Gameson *et al.* (1967) found from field observations that shoreline pollution is not significantly correlated with the onshore wind. In this section we give an illustrative example which allows us to explain why that might be the case. The example also facilitates a comparison with the computational investigation of neutrally buoyant tracers undertaken by Munro & Mollowney (1974).

We consider a steady discharge in water of constant depth, with bulk flow parallel to the shoreline, but with a wind-driven offshore drift. For a steady discharge the plume of contaminant becomes greatly elongated, and the concentration gradients

are greatest in the cross-flow direction. If the flow is principally in the x-direction parallel to the shoreline, then the two-dimensional shear dispersion equation (4.2) can be approximated:

$$\partial_x(h\|\gamma u\|\,\|c\|)+\partial_y(h\|\gamma v\|\,\|c\|)+h\|\gamma\lambda\|\,\|c\| = \partial_y(h[D_{22}+\|\gamma\kappa_2\|]\partial_y\|c\|). \quad (8.1a)$$

If there is a shoreline along $y = 0$, then the condition for no loss of tracer from the flow is

$$h\|\gamma v\|\,\|c\|-h[D_{22}+\|\gamma\kappa_2\|]\partial_y\|c\| = 0 \quad \text{on} \quad y = 0. \quad (8.1b)$$

Strictly this boundary condition (8.1b) applies on a lengthscale greater than one water depth away from the boundary. Although there can be no bulk flow $\|v\|$ across the boundary, there can be a non-zero wind drift $\|\gamma v\|$.

For water of constant depth and constant values of all the parameters $\|\gamma u\|$, $\|\gamma v\|$, $\|\gamma\lambda\|$, D_{22}, $\|\gamma\kappa_2\|$, the solution for a point discharge of strength Q at x_0, y_0 can be written as a product of a solution without decay or offshore drift, and a correction to accommodate both decay and drift:

$$\|c\| = \frac{Q}{(2\pi)^{\frac{1}{2}}\sigma hU}\left[\exp\left(-\frac{(y-y_0)^2}{2\sigma^2}\right)+\exp\left(-\frac{(y+y_0)^2}{2\sigma^2}\right)\right]$$
$$\times\exp\left[-(x-x_0)\frac{\|\gamma\lambda\|}{U}+\frac{V(x-x_0)(y-y_0)}{U\sigma^2}-\frac{V^2(x-x_0)^2}{2U^2\sigma^2}\right], \quad (8.2a)$$

with
$$\sigma^2 = 2[D_{22}+\|\gamma\kappa_2\|]\frac{(x-x_0)}{U} = 2\mathscr{D}\frac{(x-x_0)}{U}. \quad (8.2b)$$

In particular, the shoreline concentration has the x-dependence

$$\|c\|_{\text{shore}} = \frac{2Q}{(2\pi)^{\frac{1}{2}}\sigma hU}\exp\left(-(x-x_0)\frac{\|\gamma\lambda\|}{U}-\frac{1}{2\sigma^2}\left(y_0+\frac{V}{U}(x-x_0)\right)^2\right). \quad (8.3)$$

The quantity $\mathscr{D}$ in the (8.2b) is the total transverse diffusivity: shear dispersion plus turbulence.

The shoreline concentration has its maximum at the downstream location

$$x_{\max}-x_0 = \frac{\{\mathscr{D}^2U^2+y_0^2U^2(V^2+4\|\gamma\lambda\|\mathscr{D})\}^{\frac{1}{2}}-\mathscr{D}U}{V^2+4\|\gamma\lambda\|\mathscr{D}}. \quad (8.4a)$$

The maximum concentration has the formula

$$c_{\max} = \frac{Q}{(2\pi)^{\frac{1}{2}}y_0hU}\left(1+\left\{1+\left(\frac{y_0V}{\mathscr{D}}\right)^2+4\frac{y_0^2\|\gamma\lambda\|}{\mathscr{D}}\right\}^{\frac{1}{2}}\right)^{\frac{1}{2}}$$
$$\times\exp\left(-\frac{1}{2}\left\{1+\left(\frac{y_0V}{\mathscr{D}}\right)^2+4\frac{y_0^2\|\gamma\lambda\|}{\mathscr{D}}\right\}^{\frac{1}{2}}-\frac{1}{4}\left(\frac{y_0V}{\mathscr{D}}\right)\right). \quad (8.4b)$$

If we write
$$\alpha = \frac{4y_0^2\|\gamma\lambda\|}{\mathscr{D}} \quad (8.5a)$$

then the highest shoreline pollution occurs with an onshore wind drift:

$$\frac{y_0V}{\mathscr{D}} = -\tfrac{2}{3}(1+(1+3\alpha)^{\frac{1}{2}}). \quad (8.5b)$$

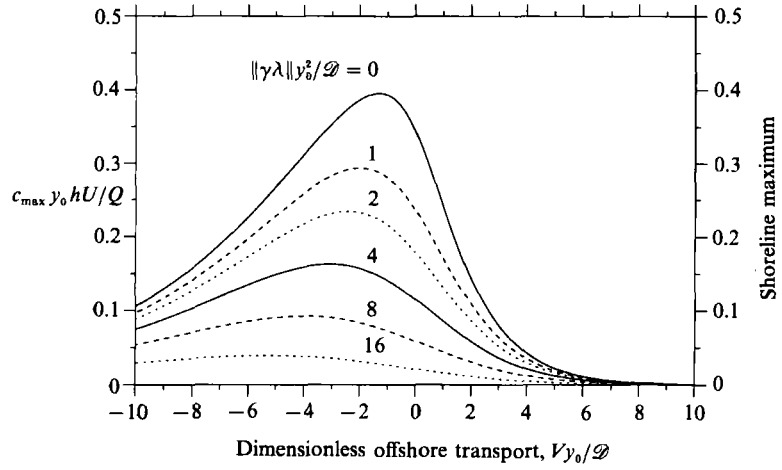

FIGURE 5. Maximum shoreline concentration as a function of the dimensionless measure $y_0 V/\mathscr{D}$ of the wind drift. Note the asymmetry between the small increase in pollution associated with onshore drift and the large reduction in pollution associated with offshore drift.

Relative to the zero-wind-drift case the highest shoreline pollution is increased by a factor

$$\frac{2}{\sqrt{3}}\left\{\frac{1+(1+3\alpha)^{\frac{1}{2}}}{1+(1+4\alpha)^{\frac{1}{2}}}\right\}^{\frac{1}{2}} \exp\left(\tfrac{1}{2}(1+4\alpha)^{\frac{1}{2}}-\tfrac{1}{2}(1+3\alpha)^{\frac{1}{2}}\right). \tag{8.5c}$$

Figure 5 shows how the shoreline pollution varies with $y_0 V/\mathscr{D}$ for several values of the decay measure $y_0^2\|\gamma\lambda\|/\mathscr{D}$. It is only over a modest (negative) range of $y_0 V/\mathscr{D}$ that an onshore drift increases the shoreline pollution. Moreover, the maximum increase for zero decay ($\lambda = 0$) is only ny a factor of $2/\sqrt{3} = 1.15$. By contrast, an offshore drift (V positive) can cause dramatic reductions in shoreline pollution.

It is the range of values of the quotient $y_0 V/\mathscr{D}$ that determines the sensitivity of the peak shoreline concentration to the wind strength. If we assume that the bulk flow is parallel to the shoreline (i.e. $\|v\| = 0$), then the effective transverse velocity V and the total transverse diffusivity $\mathscr{D}$ can be written

$$V = \frac{\hat{v}}{\exp(P)-1}\left\{\exp(P)\left[1-\frac{4}{P}+\frac{6}{P^2}\right]-\frac{2}{P}-\frac{6}{P^2}\right\}, \tag{8.6a}$$

$$\mathscr{D} = \frac{h^2 a_{\mathrm{W}}}{\kappa_3}\hat{v}^2 + \|\gamma\kappa_2\|. \tag{8.6b}$$

For weak surface drift $\hat{v}$ the magnitude of the quotient $y_0 V/\mathscr{D}$ varies systematically with $\hat{v}$ over the range

$$\hat{v}^2 < \frac{\|\gamma\kappa_2\|\kappa_3}{h^2 a_{\mathrm{W}}}, \quad \text{i.e.} \quad D_{22} < \|\gamma\kappa_2\|. \tag{8.7}$$

So, over this limited range we could expect a significant correlation between shoreline pollution and onshore wind. However, for stronger surface drift $\hat{v}$ the quotient $y_0 V/\mathscr{D}$ tends back to zero, i.e. the greatly enhanced mixing more than compensates for the increased horizontal transport of tracer. The net result would be an overall very weak correlation between shoreline pollution and onshore wind.

Munro & Mollowney (1974) neglected horizontal turbulence $\|\gamma\kappa_2\|$, integrated out the longshore x-dependence, and limited their attention to neutrally buoyant tracers

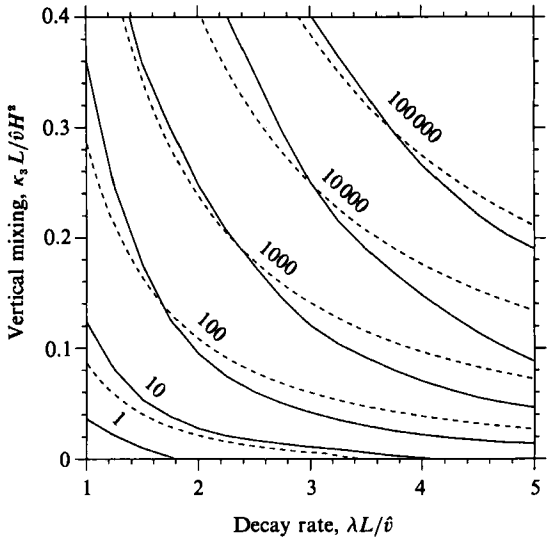

FIGURE 6. Comparison between the contours of inverse concentration computed by Munro & Mollowney (1974) for non-constant depth (solid curves), and the contours given by the solution (8.9*a*, *b*) to the advection–diffusion equation for constant depth (dashed curves). The numbers on the curves indicate the dilution factors that correspond to given values of the contaminant decay rate, and the strength of the vertical mixing.

($P = 0, V = 0$). For water of constant depth and constant values of λ and $\mathscr{D}$ the solution to (8.1) for a discharge of strength M at offshore distance L is

$$\|c\| = \frac{M}{2h(\lambda\mathscr{D})^{\frac{1}{2}}}\left\{\exp\left(-|y-L|\left(\frac{\lambda}{\mathscr{D}}\right)^{\frac{1}{2}}\right)+\exp\left(-(y+L)\left(\frac{\lambda}{\mathscr{D}}\right)^{\frac{1}{2}}\right)\right\}, \tag{8.8a}$$

with

$$\mathscr{D} = \frac{h^2\hat{v}^2}{105\kappa_3}. \tag{8.8b}$$

In particular, the shoreline concentration has the value

$$\|c\| = \frac{M}{h(\lambda\mathscr{D})^{\frac{1}{2}}}\exp\left(-L\left(\frac{\lambda}{\mathscr{D}}\right)^{\frac{1}{2}}\right). \tag{8.9}$$

To display their numerical results for the shoreline concentration Munro & Mollowney (1974, figure 32) used the combination of variables

$$\frac{M}{\hat{v}H\|c\|}, \quad \frac{\lambda L}{\hat{v}}, \quad \frac{L\kappa_3}{\hat{v}H^2}, \tag{8.10a, b, c}$$

where H is the depth of water at the discharge. The corresponding version of the above formula (8.9) is

$$\frac{M}{\hat{v}H\|c\|} = \frac{h}{H}\left(\frac{\lambda L}{\hat{v}}\right)^{-\frac{1}{2}}\left(\frac{\lambda\kappa_3}{\hat{v}H^2}\right)^{-\frac{1}{2}}\frac{1}{(105)^{\frac{1}{2}}}\exp\left((105)^{\frac{1}{2}}\frac{H}{h}\left(\frac{\lambda H}{\hat{v}}\right)^{\frac{1}{2}}\left(\frac{L\kappa_3}{\hat{v}H^2}\right)^{\frac{1}{2}}\right). \tag{8.11}$$

Munro & Mollowney (1974) considered a non-constant depth. So, in comparing the constant-depth solution (8.11) with their numerical solution we use a reference depth $h = 0.85H$ which typifies the mean depth between the discharge and the shoreline. The qualitative agreement revealed in figure 6 gives us confidence that, except for rapid decay rates or along the lower axis (where the zero vertical diffusivity κ_3 makes

it inappropriate to use vertical averaging), the horizontal advection–diffusion equation is indeed a good model for dispersion in a wind-driven flow.

When this work was begun the author held a postdoctoral fellowship funded by the Royal Society.

REFERENCES

ELDER, J. W. 1959 The dispersion of marked fluid in turbulent shear flow. *J. Fluid Mech.* **5**, 544–560.

FISCHER, H. B. 1969 The effects of bends on dispersion in streams. *Water Resources Res.* **5**, 496–506.

GAMESON, A. L. H., BUFTON, A. W. J. & GOULD, D. J. 1967 Studies of the coastal distribution of coliform bacteria in the vicinity of a sea outfall. *Wat. Pollut. Control* **66**, 501–523.

GIDDINGS, J. C. 1968 Nonequilibrium theory of field-flow fractionation. *J. Chem. Phys.* **49**, 82–85.

MUNRO, D. & MOLLOWNEY, B. M. 1974 The effect of a bottom countercurrent and vertical diffusion on coliform concentrations at the shore due mainly to wind-induced onshore currents. *Rapp. P.-V. Réun. Cons. Perm. Int. Explor. Mer* **167**, 37–40.

SMITH, R. 1983 Longitudinal dispersion coefficients for varying channels. *J. Fluid Mech.* **130**, 299–314.

SMITH, R. 1986 Vertical drift and reaction effects upon contamination dispersion in parallel shear flows. *J. Fluid Mech.* **165**, 425–444.

TAYLOR, G. I. 1953 Dispersion of soluble matter in solvent flowing slowly through a tube. *Proc. R. Soc. Lond.* A **219**, 186–203.